# 2. ACCELERATOR AUGMENTATION PROGRAMME

## 2.1 LINAC

S. Ghosh, R. Mehta, A. Sarkar, B.K. Sahu, G.K. Chaudhari, S.S.K. Sonti, D.S. Mathuria, A. Pandey, K.K. Mistri, A. Rai, J. Zacharias, P. N. Prakash, D. Kanjilal, S.K. Datta, R.K. Bhowmik and A. Roy

### 2.1.1 Simple Test Cryostat

During last academic year, several cold tests of five resonators with their respective slow tuners had been performed to make them available for the installation in linac cryostat. Slow tuner control module was used in all the tests to find out the tuning range and the mid resonance frequency of the resonators. The performance of the five resonators and their tuning range has been shown in Figures 1 and 2 respectively. In all the tests, the resonators were made to resonate at 97.000 MHz and were locked at a reasonable field by the resonator controller with the help of slow tuner control module.

Beside this main activity, simple test cryostat had been routinely used to perform pressurized helium leak test of the resonator and the burn test of the power cable inside vacuum.

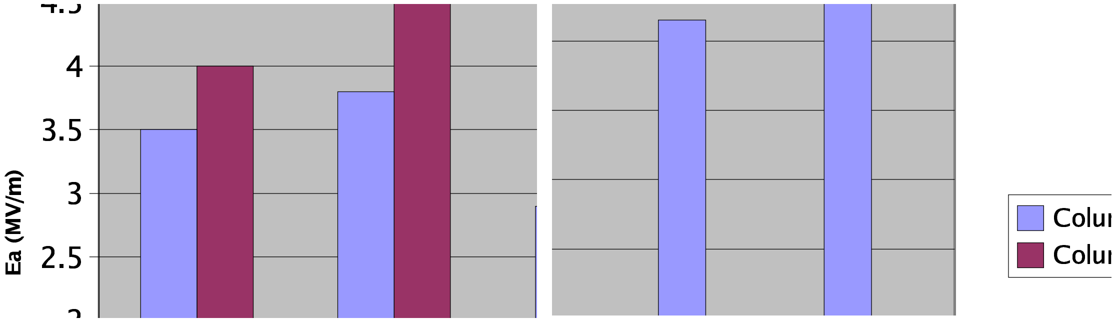

**Fig. 1: Performance of resonators @ 4 & 6 Watts of input power**

**Fig. 2: The tuning range of the slow tuner of different resonators**

### 2.1.2 Beam Test Through Linac Cavities

#### 2.1.2.1 Installation

For the test of resonators inside the linac cryostat, pickup and drive cables were laid from top of the linac cryostat up to the resonators through liquid nitrogen vessel. Pickup ports were made and loop loss was measured for all the pickups. The pickup loops were calibrated to have losses less then 2-3 mW @ 1MV/m. Variable drive probes were installed for coupling the power into the resonators and were attached to rotary motion feed throughs using universal couplings and shafts. Using this rotary motion assembly, coupling strength can be changed by moving the drive probe loop inside the resonator. All eight slow tuner lines were made, leak tested and installed.

After the installation a test was carried out to check functioning of each part. Eight resonators with slow tuners were mounted. Only two resonators were connected to drive and pickup for RF test. Test was performed with $LN_2$ filled inside $LN_2$ and LHe vessels. At this temperature we could successfully transfer and pickup the power from resonator. This test demonstrated the successful functioning of the whole setup. Later another test was carried out with liquid helium after repairing the leak observed during earlier test. In this test four resonators were mounted and 250 watts of RF power was delivered to the resonator through drive cables without any problem. Figures 3 and 4 shows the top and bottom view of four resonators and a super conducting solenoid magnet.

In beam hall II, the zero degree beam line has been extended from first LINAC cryostat to the second switching magnet. All the magnets and other diagnostic elements have been installed and properly aligned with a high precision theodolite. The cables from beam hall II to control room has been laid out for remote CAMAC control and status display of the various components up to the switching magnet. Four superconducting Niobium resonators along with a superconducting solenoid magnet had been properly aligned and installed inside the first cryostat to test their performances with beam.

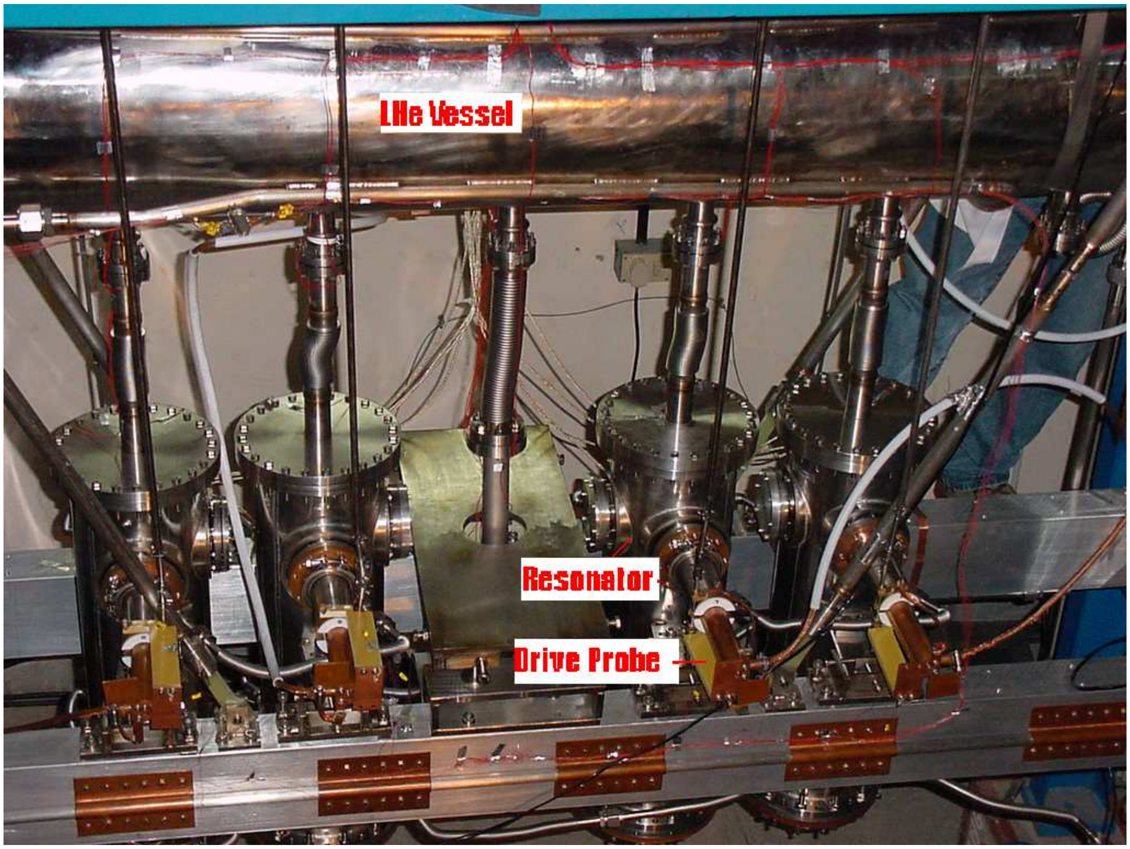

Fig.3 : Side View of Linac Cryostat

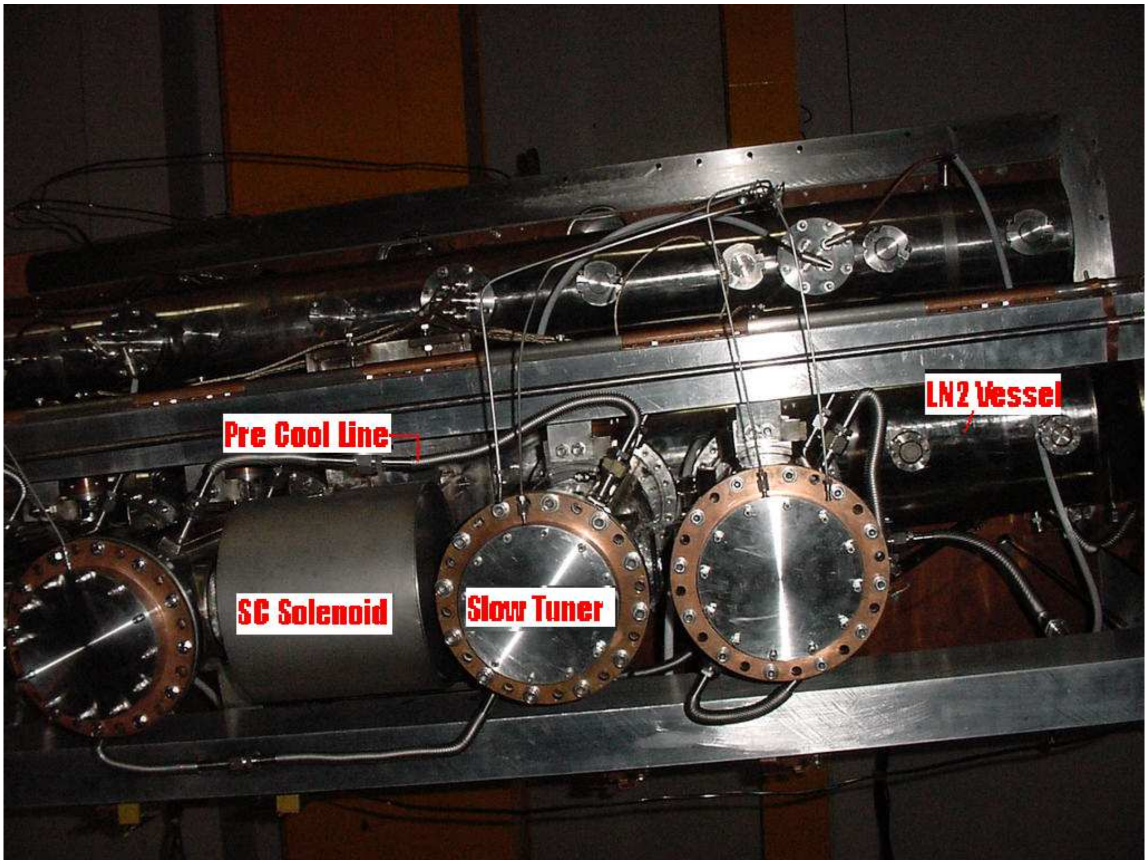

Fig. 4 : Bottom View of Linac Cryostat

### 2.1.2.2 Off Line Test

The first offline test of four resonators, inside the linac cryostat at 4.5 K, were successfully carried out by closed loop cooling through liquid helium distribution network. This test can be treated as a pre-qualifying test with respect to cryogenics, resonator performance and resonator controller electronics prior to final beam test. The performance results and the tuning ranges of the different resonators are shown in Figures 5 and 6. In this test, the minimum and maximum time taken by the different resonators for multipactoring conditioning were 21 and 53 hours respectively. There was also a substantial degradation of the accelerating field of the resonators in comparison to their results in simple test cryostat. It is believed that the resonators' poor performances were due to the absence of the magnetic shield around the resonator, contamination and perhaps some cross talk between the cavities.

The solenoid magnet was successfully energized up to 7 tesla at 4.5 K. Current was ramped up and down several times without observing any quench. Solenoid was operational up to 12 hours without any problem.

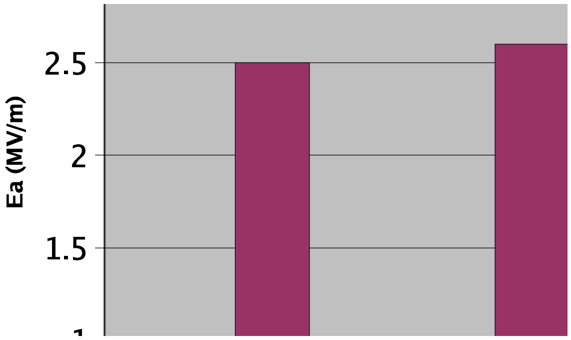

**Fig. 5 : Performance of resonators @ 6 Watts of input power**

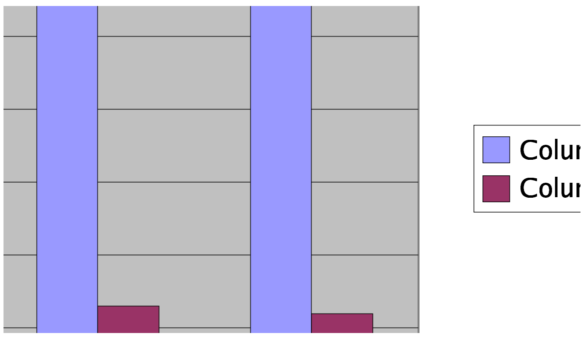

**Fig. 6 : The tuning range of the slow tuner of different resonators**

### 2.1.2.3 On-Line Test

DC nickel beam and pulsed silicon beam from Pelletron were transmitted through the linac cryostat up to a scattering chamber located at the entrance of the second switching magnet. The transmission of the beam from FC 04 in vault-I (just after the Analyzing magnet) to FC 07 in vault- II (before second switching magnet) was found to be ~ 100%.

The performance of the Multi-harmonic buncher (MHB) installed before Pelletron tank and High Energy Sweeper (HES) after Analyzing magnet was found to be satisfactory. The time structure of pulsed Si beam produced by MHB and HES was measured to be ~2 ns ( FWHM) and no drift were observed for two hours. The dark current introduced by the MHB was eliminated almost entirely by the HES. The coarse adjustment of the slits and voltage of HES had improved the peak to dark current ratio (PDR) from 60% (when only MHB is operated) to 90% (when MHB and HES both are operated). Better adjustment of the slits and voltage would improve the PDR further.

In this test 2 ns beam bunch from MHB and HES was injected into the superbuncher (SB). By adjusting the phase and amplitude of the SB a minimum time bunch of ~ 300 ps was measured at the exit of the linac cryostat. The time width of the beam bunch could not be measured at the entrance of the linac (location of optimum time bunch) due to non-availability of the detector at this location.

The bunched beam from SB could not be accelerated through the resonators in the linac cryostat due to malfunctioning of power cable and slow tuner lines. Out of four resonators mounted inside the cryostat two could not be powered due to melting of the power cables. The resonance frequency of the remaining two resonators could not be brought to 97.000 MHz due to problems in slow tuner lines. However a DC beam was injected into the working resonator and energy gain was measured. During this test it was also found that resonators had developed a leak from coupling port stainless steel bellows. Efforts are on to repair the leaks and meanwhile three leak tight resonators have been mounted in the linac cryostat. Other problems experienced in the test are fixed and a test is planed in June 2004.

### 2.1.3 Indigenous Fabrication of Superconducting Niobium Resonators

P.N. Prakash, J. Zacharias, S.S.K. Sonti and K.K. Mistri

The indigenous resonator fabrication programme has been taken up in stages. In the first stage a single quarter wave resonator was fabricated mostly out of extra parts made during the ANL project. This resonator has been successfully fabricated and tested. In the second stage fabrication of two completely indigenous resonators is presently in advanced state of completion. In the final stage production of more than a dozen resonators for the second and third linac modules would be taken up. In addition to resonator fabrication several critical repairs on existing resonators, and associated developmental work has also been done. In what follows a brief description of the entire programme is given.

#### 2.1.3.1 Indigenous Fabrication of the 1st QWR

The technology of fabricating superconducting niobium resonators is new in India, therefore this work is being taken up in a gradual manner. In order to acquire experience with electron beam welding of niobium, machining and fitting of resonator parts and sub-assemblies, electropolishing and heat treatment, we decided to fabricate the first quarter wave resonator (QWR) using extra parts that were made during the NSC resonator construction project at ANL [1]. This provided us with the opportunity to perform several critical e-beam welds and associated work and laid the road map for the second phase of construction of two completely indigenous quarter wave resonators. Figure1 shows the first resonator constructed at NSC. In cold tests this resonator performed at 4.5 MV/m accelerating electric field with 6W of RF input power (Figure 2).

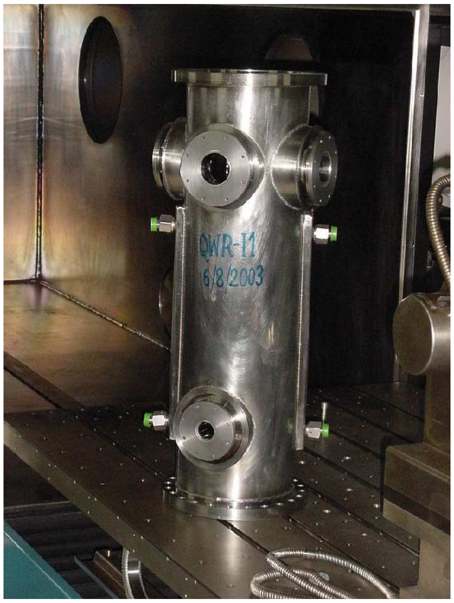

**Fig. 1: First indigenously built niobium quarter wave resonator**

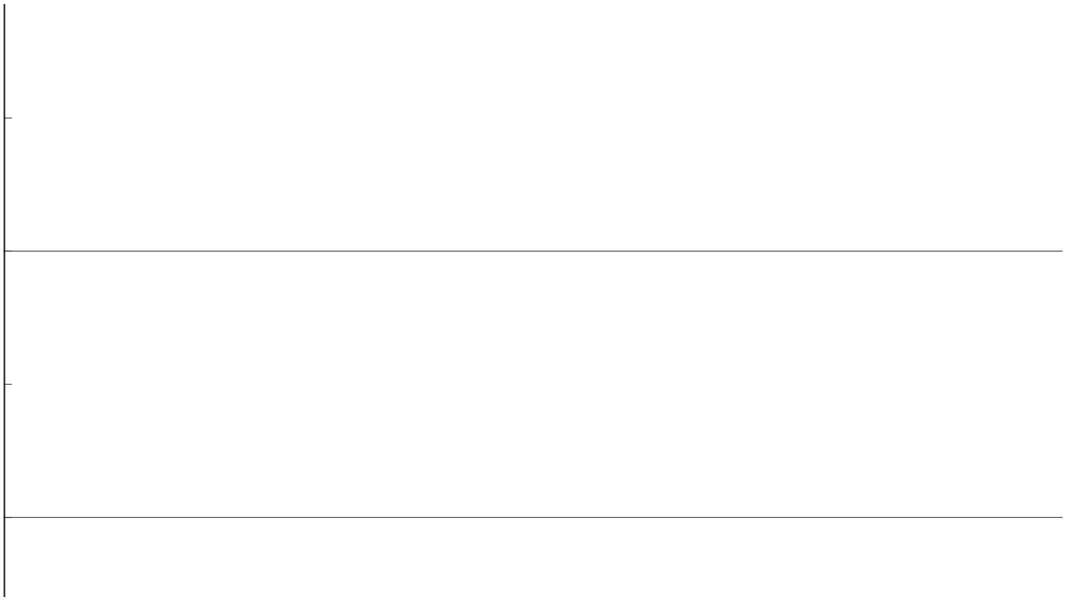

**Fig. 2: Resonator Q as a function of accelerating electric field $E_a$ at 4.5 K.**

### 2.1.3.2 Indigenous Fabrication of QWRs

After the successful completion of the first resonator, construction of two more resonators in the second stage has been taken up. Unlike the first QWR these two resonators are being fabricated completely indigenously. All machining, forming, rolling and fitting is being done at a local vendor's site and the e-beam welding, electropolishing and heat treatment is being done using the facilities setup at NSC [2]. Substantial development work at the vendor's site was undertaken to train the manpower in various machining operations and handling of niobium. Simultaneously e-beam welding parameters of those welds that were not made during the fabrication of the first resonator, were also developed. Figure 3 shows the niobium outer housings and central conductors of the two resonators ready for the closure weld. We expect to complete the fabrication in the next couple of months. Production of more than a dozen resonators for the second and third linac modules will begin after that.

**Fig. 3: Niobium outer housing and central conductors of QWR-I2 & I3**

### 2.1.3.3 Heat Treatment Getter Box

For heat treating the resonators in the high vacuum furnace [2] a niobium getter box of size ϕ 600 mm × 1000 mm out of 1.6 mm thick sheet has been fabricated. Due to the non-availability of a single sheet for rolling the cylinder of this size we had to procure two sheets of half the size (1.58 mm × 533 mm × 1829 mm) and tack them by electron beam welding. The tacking could only be done in the central one third of the sheet due to the limited chamber size and available travel in the EBW machine. The cylinder was rolled and the two halves were tacked later on. Top and bottom lids were made separately. Reinforcement was provided on the lids for weight bearing and to prevent warping. Figure 4 shows the getter box with a resonator loaded in it.

**Fig. 4: Niobium Getter box with a resonator loaded in it.**

### 2.1.3.4 Development of Transition Flange Bellows

In the NSC resonator design the transition from the inner niobium housing to the outer stainless steel jacket is provided through niobium-stainless steel explosively bonded flange and edge welded stainless steel bellows. On several of the ANL built QWRs the transition flange bellows assemblies have leaked when the resonators were loaded in the cryostat. This problem was not encountered during the prototype resonator development. In order to avoid problems on future resonators we have modified the design of the transition flange assembly using formed (instead of welded) stainless steel bellows. The wall thickness of the bellows is 0.15 mm and each assembly has four convolutions, enough to provide reasonably large stroke length and flexibility. This would avoid any stress on the ports due to differential thermal contraction between niobium and stainless steel while cooling down from 300 K to 4.5 K. Several transition flange assemblies have been fabricated, thermally cycled and pressure tested. Figure 5 shows the modified transition flange assembly for the RF power and pickup ports. The leaking assemblies on several resonators have been successfully repaired by machining them out and replacing with the modified design. Figures 6 and 7 show the coupling port before and after repairing.

**Fig. 5: Modified coupling port transition flange assembly.**

**Fig. 6: Coupling port on QWR-4 after machining out the leaking assembly but before installing the modified assembly.**

**Fig. 7: Coupling port of QWR-4 after installing the modified assembly.**

### 2.1.3.5 Repair of Punctured Central Conductor of QWR-5 & 6

Two of the ANL built resonators QWR-5 & 6, developed leak in the niobium central conductor near the top end of the drift tube. This part (called upper cap) had been die formed in two stages and we feel that during the second stage of forming it thinned down at one end due to its incorrect positioning in the die. Figure 8 shows the punctured upper cap on QWR-6. The resonators have been cut open and a new upper cap has been inserted as shown in Figure 9. This repair is rather complex since we have to maintain the frequency vis-à-vis the alignment of the beam ports of the central conductor and outer housing. The resonators are expected to be repaired by July ‘2004.

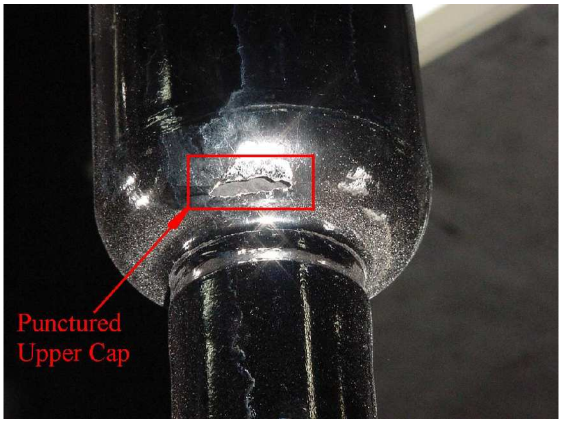

**Fig. 8: Punctured upper cap of QWR-6. The size is approximately 5 mm × 20 mm.**

**Fig. 9: QWR-6 drift tube after e-beam welding a new upper cap.**

## REFERENCES

- P.N. Prakash et al., Proceedings of the 9th International Conference on Heavy Ion Accelerator Technology – HIAT2001, PRAMANA, Journal of Physics, Vol. 59, No. 5, p. 849.
- NSC Annual Report 2002-03, p. 7.

## 2.2 CRYOGENICS

T.S. Datta, Jacob Chacko, Anup Choudhury, Joby Antony, Manoj Kumar, Suresh Babu, S.A. Krishnan, Soumen Kar, R.S. Meena, R.G. Sharma and A. Roy

In this period, first time beam from pelletron passed through the first linac module with four cavities sitting at 4.5 K. The complete cryonetwork system (Helium & Nitrogen Liquefier, Cryogen transfer line and first linac module with buncher cryostat) has been operated four times to have the beam test with linac. Each operation continued for at least a week starting from operation of helium refrigerator, cool down of linac plus buncher and finally keeping the cavities at liquid helium temperature with a constant level of liquid helium in the respective vessel. Other than this, we have also completed the additional cryogen transfer line for rebuncher and future linac cryostats. Upgradation of liquid nitrogen storage, impure helium gas storage has been initiated. Indigenously developed purifier is being operated regularly. A few experiments on heat load measurement with calorimeter have been performed and a conductivity measurement set up has been developed in this period. Brief report on major activity in the cryogenics group is presented here.

### 2.2.1 Cryogenic Facility

#### Helium Plant :

The plant was operated 8 times and out of that four in closed loop mode for linac test with beam. The total production based on engine hours (520 hours) is about 52,000 litres, which is higher than the previous two years. During this period, compressor has been operated successfully from cryogenics control room rather than compressor room by using parallel remote control panel. On average both the compressors were operated 850 hours each, which includes the recovery operation to store the pure gas in pure gas storage tank during offline testing of cavity in simple test cryostat

#### Liquid Nitrogen Plant :

The plant was operated 2718 hours and estimated liquid nitrogen production was 136,000 litters. Procurement from outside source was 96,000 litres to meet the demand of GDA and other users of NSC. Total consumption was little bit higher compared to previous year (2,00,000 litres) because of frequent linac test. Perlite insulation on condenser head of second cryogenerator was replaced with new one. Due to two phase flow of liquid nitrogen from linac shield to suction line compressor, the non return valve stopped functioning. The complete assembly was removed and the problem was rectified. To have an uninterrupted supply of liquid nitrogen for a long linac run it is planned to have an additional 20,000 litres capacity vertical liquid nitrogen storage tank. This tank is under fabrication by M/S Super Cryogenics and will be installed shortly in parallel to 5000 litres container in a new location.

#### Helium Purifier :

After the installation of the indigenously developed purifier last year, a few cycles were carried out with manual bypass option. Then the PLC controlled auto option of the purifier was commissioned. After this automatic option, the purifier has been operated successfully for ~30 cycles and approx. $3000 m^3$ of helium gas has been purified with outlet purity better than 10 PPM. After the purification cycle, the purifier undergoes regeneration and it takes ~12 hours to regenerate the system and get ready for the next cycle. The working vacuum of the system is $\sim 3 \times 10^{-7}$ torr with the turbo pump running. A flow meter is planned to be installed to measure the flow rate cum totalizer in the purifier. A gas heater will be installed in the outgoing helium line to avoid damage of the back pressure regulator down the line, which has neoprene gaskets.

#### Helium Recovery System :

The recovery compressors had been operated for 212 hours to recover the impure helium gas. Low capacity (6 $M^3$/hr. against 15 $M^3$/hr.) and higher interstage pressure were solved by complete overhauling of both the compressors. To augment the storage capacity of impure gas a single cylindrical horizontal high pressure ( 2000 psig) vessel of water capacity of 3000 litres has been designed and is in the process of fabrication.

### 2.2.2 Performance report on cooling of first Linac module with cavities

At present the buncher cryostat, first linac module and rebuncher cryostat is aligned with beam line and integrated with helium and nitrogen liquefier through indigenously developed cryogen transfer line and valve boxes. After a few trial runs on closed loop mode cooling of linac in the previous year by a different option, we have optimized the cooling methodology to reduce cool down time and to minimise requirement of cryogen. The procedure followed on cool down of LINAC is briefly reported with graphs generated by cryogenic data acquisition and control system (CRYO- DACS).

Once linac vacuum at room temperature is better than $10^{-6}$ torr, shield cooling is started with an optimum flow of 20 litres/hr. $LN_2$ along with baking of cavities. Baking is stopped after 24 hours. After 72 hours of shield cooling, the inside enclosures consists of cavities, dewar and support structure achieve temperature of approx. 230 K through radiative cooling. The cavity temperature is further reduced to approx. 140-150 K by precooling with liquid nitrogen through the precool line @ 15 litres/ hr.

The helium plant is started in parallel with dewar in warm condition. Once the dewar achieves a temperature approx. 40 K, part of cold gas after JT is diverted to Linac through distribution line. Return warm gas from linac is connected to suction line through heater and turbine flow meter till it attains 20 K at the outlet. Once return temperature is below 20 K, return flow diverted to helium dewar by opening return valve and flow rate is enhanced by opening further supply valve in valve box 1. The helium vessel reaches 4. 5 K in 4 - 5 hours as against 20 hours for the cavities as cold helium gas is not circulated through cavities. Once the cavities reach 4.5 K, the bypass valve is almost closed to divert the full liquid to linac and collect liquid He. This process continued till liquid helium level rises to 90 – 100%. Then buncher supply valve is crack opened and linac supply valve is partly closed to cool the buncher cavity. It takes only 3-4 hours to cool the buncher cavity.

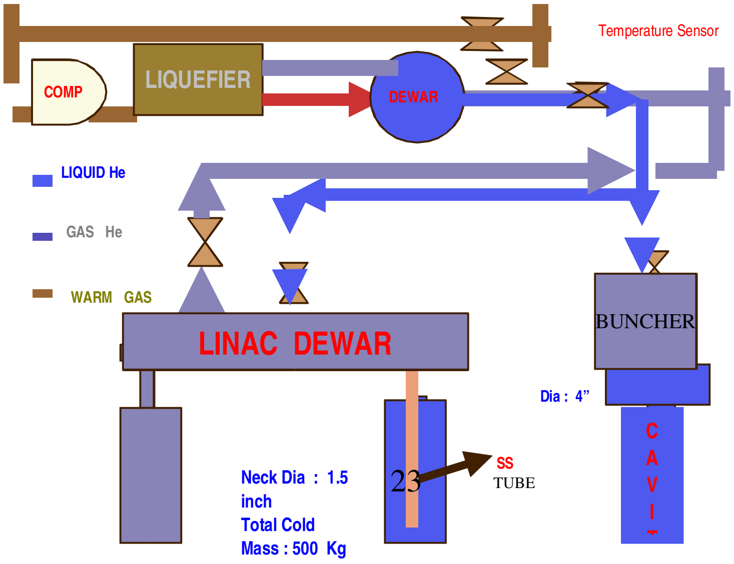

**Fig. 1: Cooling schematic of LINAC**

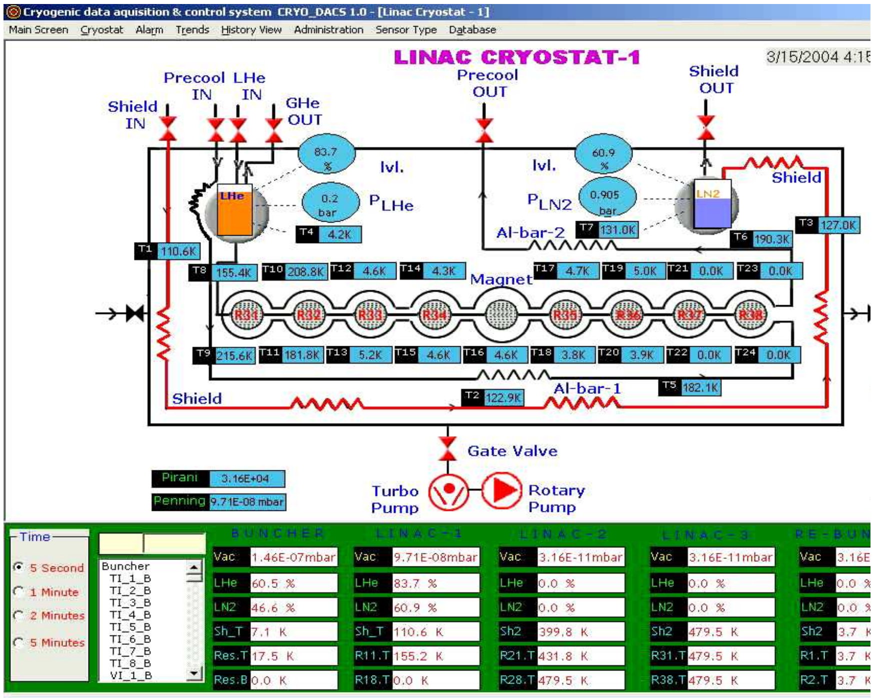

Pirani 3.16E+04
Penning 9.71E-08 mbar

● 5 Second
○ 1 Minute
○ 2 Minutes
○ 5 Minutes

| BUNCHER | | LINAC-1 | | LINAC-2 | | LINAC-3 | | RE-BUN | |
|---|---|---|---|---|---|---|---|---|---|
| Vac | 1.46E-07mbar | Vac | 9.71E-08mbar | Vac | 3.16E-11mbar | Vac | 3.16E-11mbar | Vac | 3.16E |
| LHe | 60.5 % | LHe | 83.7 % | LHe | 0.0 % | LHe | 0.0 % | LHe | 0.0 |
| LN2 | 46.6 % | LN2 | 60.9 % | LN2 | 0.0 % | LN2 | 0.0 % | LN2 | 0.0 |
| Sh_T | 7.1 K | Sh_T | 110.6 K | Sh2 | 399.8 K | Sh2 | 479.5 K | Sh2 | 3.7 |
| Res.T | 17.5 K | R11.T | 155.2 K | R21.T | 431.8 K | R31.T | 479.5 K | R1.T | 3.7 |
| Res.B | 0.0 K | R18.T | 0.0 K | R28.T | 479.5 K | R38.T | 479.5 K | R2.T | 3.7 |

**Fig 2 : Data sheet on linac as it appears on CRYO-DACS during LINAC run**

We found that the Aluminium support bars attain equilibrium temperature of 130 K, although cavities are kept at 4.5 K for 7 days, giving a continuous heat leak at 4.5 K.

We are able to maintain the LHe level by running one compressor in place of two, considering the load only from one linac, buncher and distribution line. We find that the time to fill liquid helium in linac cryostat is approximately 24-30 hours starting from helium plant operation.

### 2.2.3 Extension of LN2 transfer line and Rebuncher helium line

Second phase of distribution line has just been completed. In this phase provision for LN2 cooling has been included for simple test cryostat (STC), LINAC 2, LINAC 3, and rebuncher cryostat (RBC). Also provision has been kept for manual filling of small stand alone dewar in the beam hall 2. To distribute LN2 in all these application sites, modular valve box approach has been adopted. Each valve box consists of 2 cryogenic valves, two indigenously developed bayonet connections, one pump out port and a provision for gauge connection. All these bayonet connections are at present blanked off except VB-5, from where Rebuncher cryostat shields are being cooled through stand alone transfer line. Total length of the distribution lines is 45 meters. The inner line is of ½”NB x sch5 and the outer line is 2”NB x sch5. Inner line is wrapped with 12 layers of Jehier made super insulation. The distribution vacuum line is bifurcated into two parts with a vacuum break between VB-3 and VB-4. Also we have added appropriate amount of charcoal in the inner line to enhance the cold cryosorption capacity.

During the execution of the project a detailed leak testing of the system has been carried out starting from the valve box, the individual lines and finally to the whole system. After the completion of the transfer line a detailed helium leak test was carried out with inner line pressurized by helium gas at 60 psi. After that the system underwent extensive baking, where hot gas was passed from inside tube and outer pipe warmed with tape heaters. This takes care of the embedded moisture and hydrogen in the vacuum system. After attaining vacuum better than $5 \times 10^{-4}$ torr the whole system was cooled down and the vacuum locked.

**Fig. 3 : Inside of LN2 Valve box** **Fig. 4 : Series of valve boxes**

Vacuum retention test continued thereafter for 10 days. At the completion of the retention test whole of the set up was cold shocked with LN2 over a period of a week.

Apart from this LN2 distribution line, liquid helium line connecting the rebuncher cryostat to helium VB-4 has been completed. In this case the inlet and outlet lines are of ½"NB × sch5 and the outer line is 5"NB × sch5. Vacuum break in the valve box side was provided with 1.5" dia × 18" long MDC vacuum bellow. Each of the inner lines has a demountable section with Cajon fittings connection each end. This helps us to move cryostat safely without damaging the end coupling. On the vacuum flange part both o-rings has been placed in a half dovetail groove in the corresponding flanges, which help in the retention of the ring, and at the same time the groove configuration ensured positive vacuum sealing. A single ply 5"NB bellow on the outside takes care of small misalignments.

### 2.2.4 Cryostats

Linac cryostat with aligned cavities and superconducting solenoid along with all accessories like RF power cable, pick up cable, slow tunes assembly were tested with beam. Precool line of linac has been modified with vacuum jacketed line and control valve to have optimized flow to precool the cavities from 220 K to 140 K. Similarly an additional control valve with lower Cv value is integrated in the transfer line connecting the valve box and linac cryostat for shield cooling.

**Alignment of the cavities and solenoid magnet in Linac cryostat :**

To take the accelerated beam out of the cryostat, the alignment of the cavities are very important. The outer vacuum jacket of the cryostat is placed in the beam line and aligned with respect to the beam. Cavities are mounted on the top plate and alignment has to be done while the top plate is resting on a special stand designed for this purpose.

The first task is to transfer the beam axis to the top plate assembly while it is resting on the stand. Special fixtures are mounted on the top plate assembly and transferred the beam exit and entry points to this fixture after placing the top plate assembly on the outer vacuum jacket. Then transferred the top plate assembly to the special stand and aligned the Theodalite with respect to the beam axis on the fixture.

On the cavities, supports were welded to clamp it on the specially designed alignment mechanism. By this mechanism each cavity can be moved in X Y Z directions independently. The position of the cavity beam port with respect to the beam line axis also can be adjusted vertically. By this method four cavities were aligned and tested with beam.

Another important component is the super conducting solenoid magnet. Alignment of this is also very critical for the successful extraction of the beam. A different alignment mechanism is developed for this purpose and is shown in Figure 5.

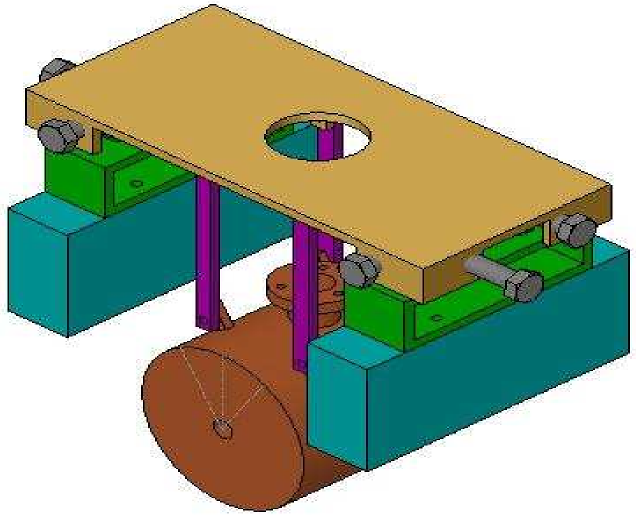

**Fig. 5 : Magnet support & alignment system**

### Buncher, Rebuncher and Simple Test Cryostat

Buncher cryostat was opened once to change the faulty RF cable and to have better cooling mechanism to transfer the joule heating of cable either at LN2 temperature or helium temperature. After insitu cleaning and water rinsing, the cryostat was reloaded again for beam testing.

Rebuncher cryostat was aligned with respect to beam line and beam axis has been transferred to inner assembly by welding a fixture on the helium vessel. This has been integrated with valve box by a demountable 5 inches dia. vacuum-jacketed multilayer insulated line. Rebuncher cryostat is equipped with conventional annular liquid nitrogen shield with two parts. Both these vessels are connected to liquid nitrogen valve box through Bayonet connection. Performance test at liquid helium temperature was satisfactory and the cryostat is ready for loading cavities.

Simple test cryostat was used at least four times to have the performance test of cavities including the indigenous cavity. Recently a permanent liquid nitrogen line has been connected to have online filling of liquid nitrogen from main tank.

### 2.2.5 Miscellaneous work

#### Experiments on MLI Set up

Last year it was reported about extraneous heat transfer through angular radiation from top plate. To have a detailed analysis on angular radiation contribution a series of experiments were conducted with various dimensions copper shield attached on guard vessel. Although the heat load reduced significantly (from 400 mw to 50 mw), the source of residual heat leak is not identified clearly. The summary of the experimental results is reported here. Geometry factor or view factor is being calculated to have the understanding of angular radiation contribution.

| **Heat load At 80 K** | **Without shield** | **240 mm dia. shield** | **260 mm dia.** | **280 mm dia.** |
|---|---|---|---|---|
| Bare Surface | 360 mw | 300 mw | 220 mw | 103 mw |
| With 5 layers of MLI | 200 mw | 184 mw | 95 mw | 46 mw |

Various possibilities of heat leak like conduction load through sensor lead, joule heating and radiation /convection load along the ½ inches dia pipe contributing to the residual load were considered and found insignificant. For the experiment with liquid helium for different insulations, it is planned to have a copper shield at the top to minimize the residual heat load.

#### Experimental set up to measure thermal conductivity in the temperature range (4.2 K to 300 K )

We have a long term plan to establish a low temperature (4.2 K – 300K) measurement facilities with and without magnetic field to measure thermal conductivity, electrical resistivity, RRR etc for the materials used for our LINAC programme. In this year we have developed two cryostats of dip stick type that goes into a 100 mm diameter neck of liquid helium container. In this set up thermal conductivity is measured by establishing a steady temperature gradient along the sample by using a heater at one end of the sample. The temperature of the sink is maintained constant by a Lakeshore temperature controller.

**Development of Cryogenic valve**

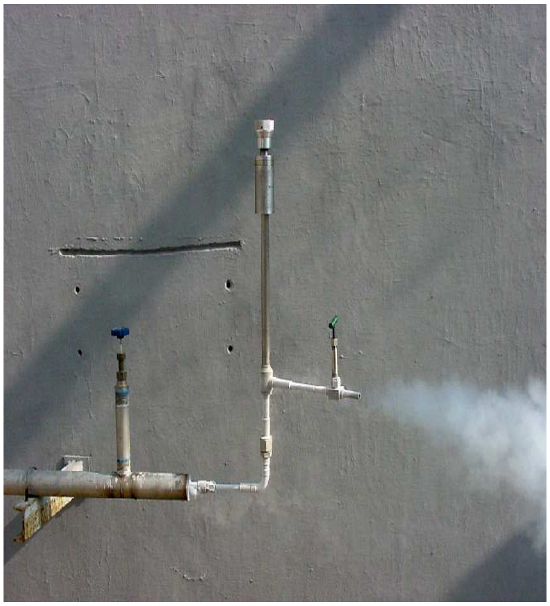

Fig 6 : Cryogenic valve developed at NSC

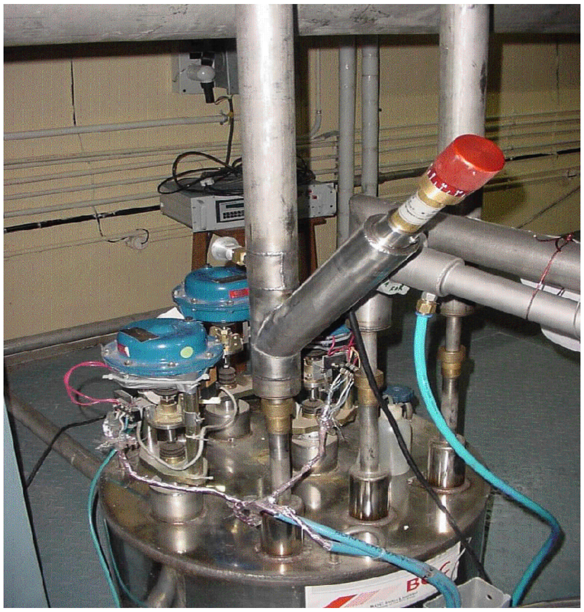

Fig 7 : Fine control valve for Linac shield

A long stem cryogenic valve has been fabricated keeping in mind the necessity of the future use and specially non-availability of these in our country. The cold sealing of the valve is with Teflon and the warm seal is with double o-ring. The orifice of the valve is a 15 mm dia. hole. After fabrication, it has undergone numerous leak test and cold shocks with LN2. The room temperature leak rate across the cold seat is found to be ~ $10^{-6}$ torr. lt / sec, which is well with the acceptable limit of bubble tightness. Some further cold shocks are planned to be done over the next few months and leak rate at cold condition will be determined.

### 2.2.6 A Linux Based Control and Data Acquisition for the Automation of a Surface Preparation Facility Using Ni Field Point Hardware

Joby Antony

A surface preparation facility, which demands a high degree of safety, has been completely automated to electropolish Superconducting resonators at NSC and is presently under operation. The hardware used is NIT Field point modules accessed from a linux OS for controls & data acquisition which assured continuous error free operations. The various mechanical components of this unit are a CHILLER, ACID PUMP, 1000 A power supply, BLOWER FUME HOOD etc. The time varying current, approx. 700 A max. across two electrodes inside a mixture of sulphuric and hydrofluoric acid is controlled and measured for slow realtime operation from a PC. The duty cycle and number of cycles are programmed according to the setup. The acid temperature is measured using a teflon coated PT100 sensor immersed in acid. The home made controller displays the temperature in deg. C and also gives a 0-10 volts for interfacing AI 110 to measure online temperature every second. The CHILLER UNIT is ON/OFF controlled within a software LLT and ULT temperature setpoints through FPDO. The ACID PUNP is made ON and OFF to circulate the acid only during the off time of power supply to prevent saturation. The FUME HOOD door and BLOWER is interlocked to ensure the accident free operations. The LINUX based GUI is developed using C++ based Qt tool kit from trolltech. All the analog and digital ip data are recorded every second. The online and offline data plots are achieved by using gnuplot. Multiport serial programming has been done with a LinSerial class for serial interfacing FP modules and power supply. The control and monitoring both can be done from any machine within NSC LAN remotely. The automated system runs for 5-6 hours continuous for a complete electropolish cycle making the operation simple and safe.

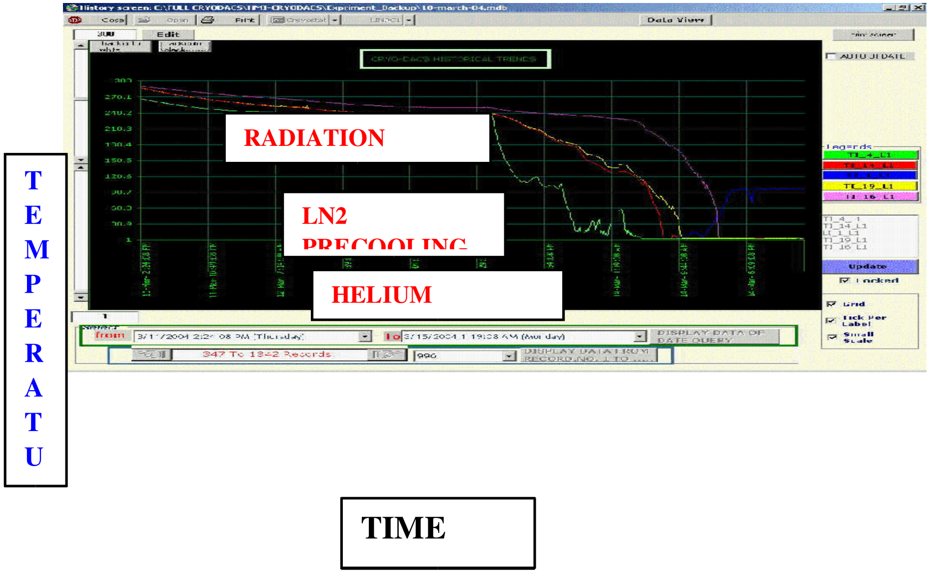

**Fig 8 : Complete cool down profile of LINAC cavities and magnet.**

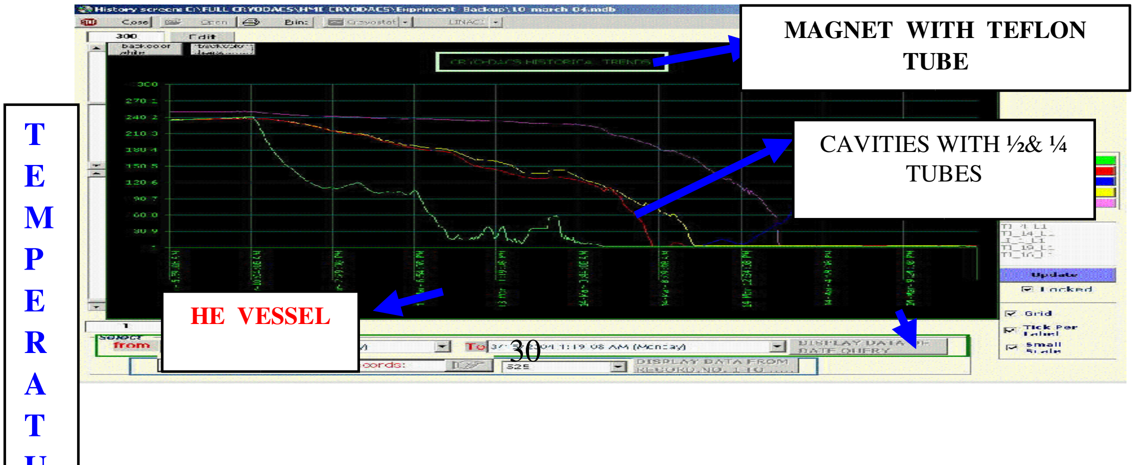

**Fig 9 : Comparison of cooling rate of cavities and magnet**

## 2.3 RF ELECTRONICS

Ajithkumar B.P., A. Sarkar, B.K. Sahu, K. Singh, S. Venkataramanan,
R. Shanthi and A. Pandey.

### 2.3.1 Status of LINAC Control system

Electronics required for controlling eight resonators have been installed in the new beam hall and tested. The 400 Watts VHF power amplifiers required for powering the resonator were developed inhouse and ten numbers of the same has been produced by BEL, Bangalore. Six pieces of 250W amplifiers were also fabricated inhouse and installed in the beam hall. Ten pieces of the resonator control modules were supplied by BARC and are installed and tested. The CAMAC interface module for controlling these modules from the computer has been developed inhouse. Ten such modules are being installed and tested.

The computer control system has been augmented to support the LINAC and multiple operator consoles. CAMAC Crate controller with built-in computer running Linux operating system was developed inhouse. Ten such modules are being deployed in the control system. The other CAMAC modules like ADCs, Output registers, Input Gates etc. also has been developed and deployed.

The electronics and mechanical assembly required for controlling eight resonators and superbuncher have been installed and tested.

### 2.3.2 Status of Multi-harmonic buncher and High Energy Sweeper

The Multi-harmonic buncher (MHB) was operated along with the High energy Sweeper (HES) for the first time to provide pulsed beam to the Linac beam line. $^{28}$Si beam bunches of ~1.5 ns FWHM were produced by the MHB. The dark current between bunches was cut down by 90% by the HES after proper adjustment of the sweeper slits. The system was quite stable for long duration. At times due to severe phase drifts in the Pelletron beam, the system went out of lock and the phase of the sweeper had to be adjusted to bring the lock back.

The old beam pulsing system supplied by NEC, consisting of a chopper and a single frequency buncher, provides pulsed beam at 4 MHz. But it has no phase locking with beam. Due to phase drift in the Pelletron beam it became quite difficult for User's to run pulsed beams for long duration. On the other hand the new beam pulsing system, consisting of the multi-harmonic buncher and high energy sweeper, is phase locked with the beam and provides pulsed beam at 12MHz (mainly to be used for Linac). Since most user experiments need pulsed beams at 4 MHz or a submultiple of it, the new beam pulsing system could not be used directly. It was thought of integrating the chopper of the old pulsing system with the multi-harmonic buncher in order to provide phase stable 4MHz pulsed beam to the users. In order to do this, a 4 MHz clock was generated from the 12MHz MHB master clock and was used to drive the chopper. Phase of the chopper was adjusted externally to match the MHB phase.The system worked quite satisfactorily and provided $^{7}$Li, $^{12}$C, $^{16}$O, $^{19}$F, $^{28}$Si, $^{31}$P stable pulsed beams to several users.

## 2.4 BEAM TRANSPORT SYSTEM

A. Mandal, Rajesh Kumar and S.K. Suman

Beam transport system carries the responsibility of maintenance of the existing beam transport system. Simultaneously this group has undertaken the following development project.

### 2.4.1 Super Conducting Solenoid Magnet Power Supply and Programmer Testing

Rajesh Kumar

A prototype power supply and programmer had been designed. Last year five sets of such power supplies and programmers got fabricated and tested thoroughly. At present one power supply has been installed at Material Sc. Lab for charging 8T super conducting magnet and one set installed in PH-II for LINAC Module-I. Following test have been carried out:

- Local operation
- Remote operation- current setting (0-5V), current read (0-5V), four status signal Power test at 80A/10V
- Load and line regulation -0.1% for 10% change
- Output ripple- 100mVpp
- Stability - 600ppm (0.06%)

### 2.4.2 Super Conducting Solenoid Magnet Power Supply Controller

S.K. Suman and A. Mandal

After successful development of super conducting solenoid magnet power supply, a CAMAC based controller has been developed for remote controlling the super conducting magnet power supply. Last year, five numbers of such modules have been developed, fabricated in house and tested. The module have a 16 bit DAC to set the power supply current, 12 bit ADC for monitoring super conducting magnet current, 4 bit input gate for status read of magnet and power supply.

### 2.4.3 16 Bit Input Gate Output Register (IGOR)

S.K. Suman and A. Mandal

CAMAC based IGOR module is an in house development and in use since last two years. This module controls the magnet power supply in remote operation. Last year, ten numbers of such modules have been fabricated and tested. These modules have been installed in PH-II beam lines.

### 2.4.4 High Current High Stability Power Supply (300A/100V, 10 ppm)

Rajesh Kumar, Raj Kumar, Bishamber Kumar and A. Mandal

A prototype power supply has been designed for HYRA Quadrupole magnet. As the output current and voltage both are high (300A/100V), so at the input side pre regulation technique is used to minimise the power dissipation across the transistor bank. It is a linear current regulated power supply based on series pass technology. A temperature compensated double loop regulation system is used to cover a wide range of inductive loads. Following sub assemblies have been developed:

- 43 kVA 3-Phase auto transformer
- 43 kVA 6-Phase doubled delta transformer
- 6-Phase water cooled rectifier with high frequency filtering
- 35 mF capacitor bank for a max. ripple of 7% at 300A
- Designed and assembled a water cooled 7kW, 300A rating transistor bank with hfe 3000. Transistor fail indication and detection circuits incorporated
- Magnet time constant corrector and back emf protection
- Vario transformer control circuit
- LC filter module for a ripple of 7% at 300A./100V. The resonance frequency is kept around 74 Hz to pass all the 50 Hz and multiples
- Previously assembled electronics is used and scaled for over current, load line, Common emitter voltage, transistor fail, output voltage, output current to interface with the increased power

All above modules/part have been housed in 19" rack and wired. Power supply has been tested at 75Amp. Performance testing to be done at maximum rated current.

### 2.4.5 NIM Based 5kV/100μA Programmable Ge Detector Bias Power Supply

Rajesh Kumar, A. Jhingan and A. Mandal

A NIM based high voltage power supply has been developed for biasing Ge detectors. The power supply control is based on SMPS technique. 24V DC is chopped and step-up to 360V and then multiplied by a 14 stage cockroft-walton half wave voltage multiplier to get 5 kV. Power supply has following controls and features:

- Over load shut down
- Power fail reset
- Polarity selection - internally

- Detector cooling shutdown
- Output can be ramp up and down with programmable ramp rate and can be paused.
- Automatically go to ramp down mode when ever shutdown
- Ready signal available when set value is achieved
- 0-5V signal for 0-5 kV output at front panel for Vo monitoring

Performance testing carried out and found 0.2% voltage stability at 100µA with constant temperature, load and supply voltage.

### 2.4.6 Prototype Development of Air Cooled 1kW (30V/35A, 25ppm) Power supply:

S.K. Suman, Rajesh Kumar and A. Mandal

At present we are using water cooled high stability power supply. A project has been under taken to develop air cooled high stability power supply for HCI quadrupole magnet. Control electronics has been developed and tested. Final assembly is in progress.

### 2.4.7 Development of Remote and Local Control Interface for ±50 kV Wien Filter Power Supply

Rajesh Kumar, Suraj Kumar and S.K. Datta

A remote and local control interface module has been developed for Wien filter power supply. Two nos of 50kV modules from Glassman has been used to fabricate ±50kV power supply. Following features provided in the module:

Local interface:

- provide Vo and Io display using DPM
- Vo and Io control using 10T pot
- LED's status display on front panel
- Remote/Local selection switch
- Master/ Slave function for tracking
- Enable/Disable switch

Remote control is done through 25 PD connector for Vo control (0-10V), Vo read (0-10V), opto isolated status read.

## 2.5 LOW ENERGY ION BEAM FACILITY

G. Rodrigues, P.Kumar, U.K. Rao , C. P. Safvan and D. Kanjilal

### A. Source operation

During last year, the source has been running for an appreciable amount of time on the development of metal ions by using the micro-oven and MIVOC (Metal Ions using Volatile Compounds ) technique. The source has been working satisfactorily with reasonable amount of currents required for experiments related to materials sciences, atomic and molecular physics. However, from source development point of view, the beam currents are limited due to various reasons related to transmission problems through the beamline. In this direction, the transmission from the source through the beamline is being improved in many possible ways. One of the possible improvements is to maintain better focussing properties at the object plane of the analysing magnet. This could be possibly realised by incorporating two strong focussing elements; one between the high voltage accelerating tube and the object slit and the other between the source and the high voltage accelrating tube. This work is currently in progress.

A new system (shown below in Figure 1.) was developed for extracting metal ions using the MIVOC technique which were not possible with the existing oven system. The aim of the present system was to improve the conductance by coupling the MIVOC chamber as close as possible to the source and to facilitate ease in tuning of the flow of the vapour similar to the case of gases. It consists of a small MIVOC chamber connected to the injection side of the source through a vapor flow control valve which controls the flow of the vapour into the source. The system was succesfully tested by extracting Fe beam using ferrocene compound [$Fe(C_5H_5)_2$] which has a vapor pressure of $1.7\times10^{-3}$ torr at 20ºC. In another experiment, Si was extracted using chlorotrimethylsilane [$Si(CH_3)_3$ Cl]. Some of the other metal beams developed using the micro-oven were As, Ge and Zn.

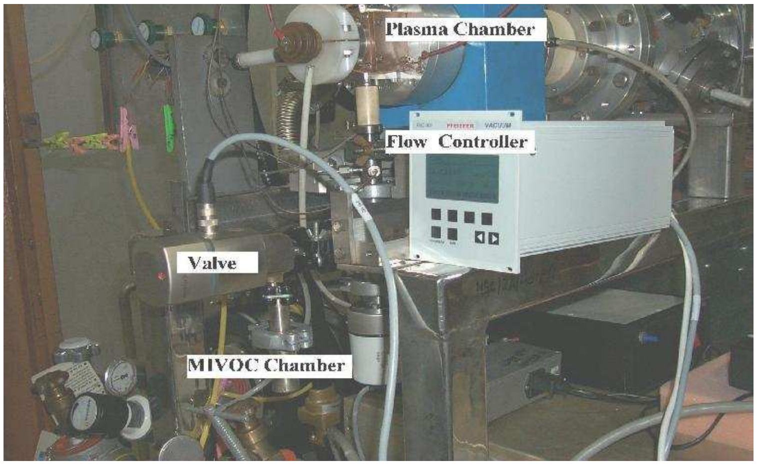

**Fig. 1 : MIVOC system coupled close to the NANOGAN source**

The following experiments were performed in materials sciences beamline using Xe, Ge, Fe, N and O beams at various energies varying between 50 keV to 1 MeV.

1. Mixing of Au/Ge multilayers, bilayers and monolayers on Si substrate
2. Production of Ge nanoparticles on oxidised Si and $SiO_2$ wafers
3. Fe implantation on $Li_2O$-$B_2O_3$ glassy system for optical and electrical studies
4. Fe implantation on quartz, glass and saphire
5. Synthesis of Silicon oxynitride buried layers

6. Ion beam induced epitaxial crystallisation

## B. 15º beam line at the low energy ion beam facility (LEIBF)

G.K.Padmashree[1], C.P.Safvan, G.Rodrigues, U.K.Rao, Pravin Kumar, R.Ahuja, Sunder Rao, J. Zacharias, S.K. Saini and D. Kanjilal

[1]Department of Studies in Physics, University of Mysore, Manasagangotri, Mysore - 570006

A new beam line (15º) for experiments with liquid droplets and atomic/molecular clusters has been developed recently at the LEIBF, and has become operational of late. The beam optics has been designed so as to obtain a m/q selected and doubly focussed low energy highly charged ion beam with unit magnification, at the center of the experimental chamber. The code for beam optics simulation was written in-house. The following figure shows the simulated beam envelop for an ion beam with 100 keV energy per charge state.

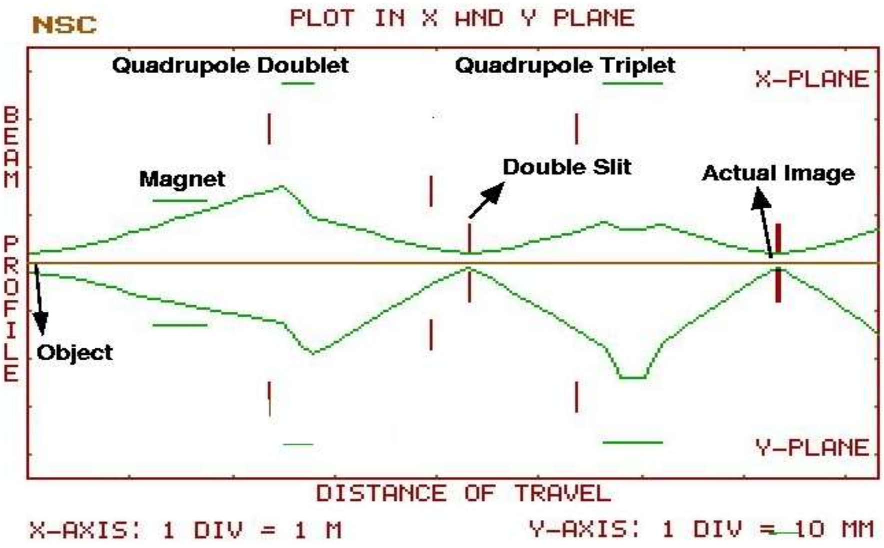

**Fig. 1: Simulated beam envelop in the XZ and YZ planes for a beam with E/q = 100 kV traveling through the 15º beam line (along Z axis)**

This beam line is unique in the sense that it constitutes a combination of a dipole magnet (analyzing magnet) and an electrostatic quadrupole doublet, together with an electrostatic quadrupole triplet for obtaining a doubly focussed beam after the magnet as well as at the target location. The electrostatic quadrupoles (doublet and triplet) that are used for beam focussing, have been indigenously fabricated, and so is the electrostatic steerer that allows for beam steering. The high voltage feed throughs for the quadrupoles and steerers have been fabricated in-house. The commercially available beam diagnostic elements like beam profile monitor (BPM) and Faraday cup have been incorporated at suitable positions along the beam line. A manually-operated double slit allows for cropping the peripheral beam. Rotary-backed turbo-molecular pumps have been installed at different positions along the beam line for achieving and sustaining ultra-high vacuum, and appropriate gauges have been used for pressure diagnostics. In order to ensure faithful transmission of the beam, all the above components together with the drift tubes and bellows, have been aligned with an accuracy that is better than 0.5 mm.

**Fig 2: Photograph of the 15° beam line.**

The high voltage power supplies (for quadrupoles and steerers), pump/gauge controllers and the interfacing modules (Field Point) are housed conveniently below the beamline. The power supplies for the quadrupoles are remote controlled through RS232 interface. Beam tuning for maximum transmission with best profile, is done through a user-friendly control software. The performance of the line has been tested out by actually performing a beam test with $Ar^{2+}$ beam at 200 keV energy, and the results have been very satisfactory.

### C. A novel experimental setup for HCI-liquid droplet interaction studies

G.K. Padmashree[1], R.Ahuja, C.P. Safvan, Sunder Rao and A.Roy

[1]Department of Studies in Physics, University of Mysore, Manasagangotri, Mysore - 570 006.

The studies on interaction of liquid droplets with low energy highly-charged ions are radically new, and experiments to understand the dynamics of such an interaction have been initiated by us. To the best of our knowledge, such experiments are being carried out for the first time anywhere in the world, and a novel experimental setup for the same has been developed at the LEIBF.

The setup constitutes an UHV experimental chamber which is installed at the end of the 15° beamline at the LEIBF. It houses a modular cryopumping system and a differential pumping system apart from the conventional high-capacity pumps (rotary-backed diffusion pump), for achieving and sustaining high vacuum when the liquid droplets are introduced. A flexible bellow arrangement at the top of the chamber for mounting the piezocrystal driven microcapillary tube, allows for aligning the droplet train with the ion beam. A Wilson-seal arrangement that is coupled to the bellow on one end and firmly held by a rail support on the other end, facilitates vertical movement of the capillary.

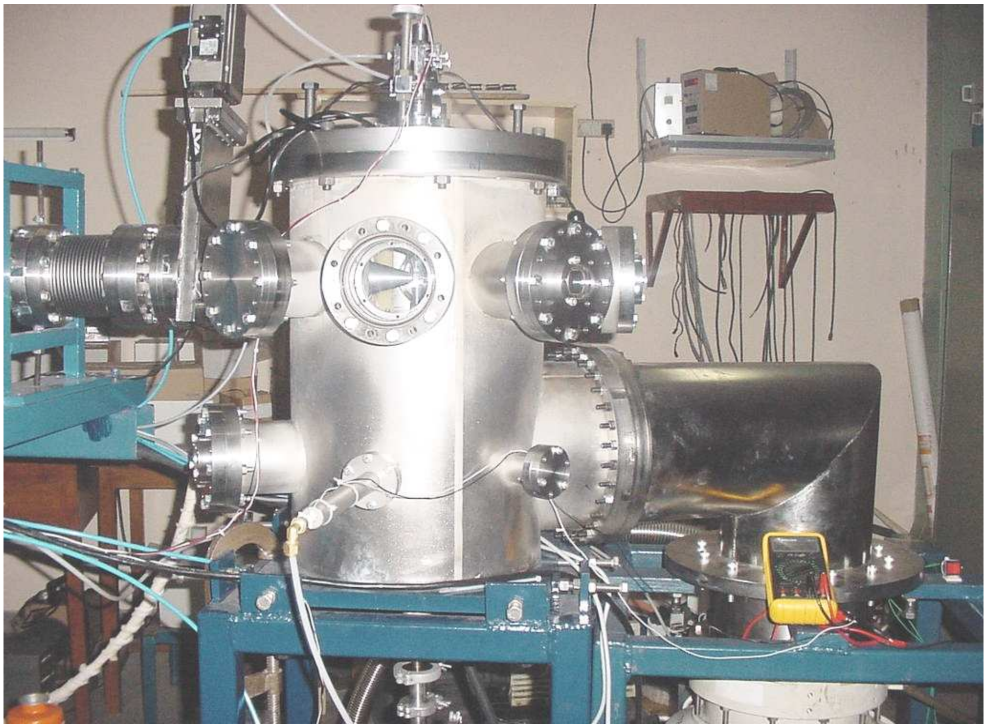

**Fig 1: Experimental chamber along with the capillary housing arrangement**

The differential pumping arrangement in the form of a cone on the beam-entry side of the chamber ensures minimal degradation of the beam line vacuum. A 2mm hole near the vertex of this cone acts as a conductance limiter and a beam collimator. The cryopumping system provides about 6000 $cm^2$ of liquid nitrogen ($LN_2$)-cooled copper surface for the evaporated liquid target and also serves to trap the oil remnants from the diffusion pump, thereby sustaining good vacuum in the chamber. While the $LN_2$ 'in and out' of the copper coils (inside vacuum) is through a double walled tube, thermal and electrical insulation otherwise is ensured by mounting the copper coils on G10 insulator. An arrangement to measure the temperature of the $LN_2$-cooled coils has been made.

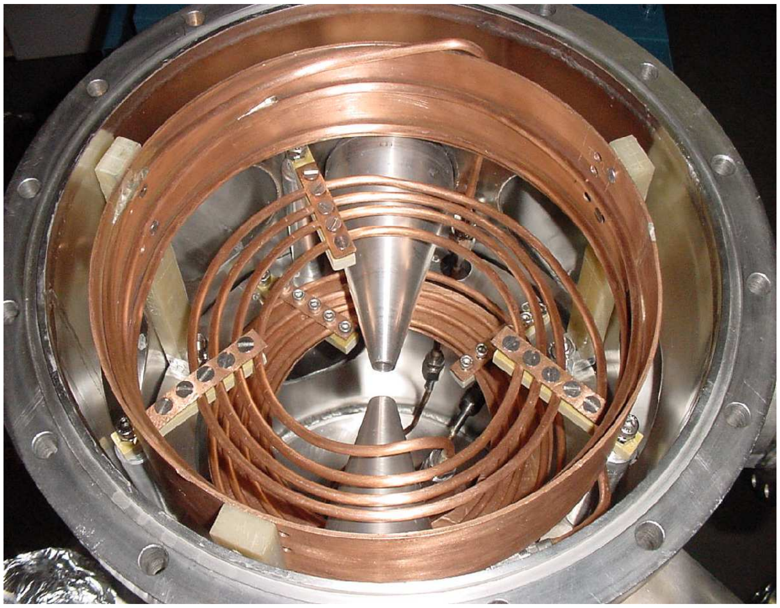

**Fig. 2 : Cryopumping and differential pumping system inside the experimental chamber**

A special arrangement for collecting the direct droplet train and pumping it out through a rotary pump has also been made. All the conventional pumps together with the isolation valves, are operated through an electronic interlock system. The chamber has a number of ports around the interaction region so as to accommodate photon and particle detectors. A special re-entry cup with 20 micron-thick mylar foil is coupled to the chamber for mounting x-ray detectors very close to the interaction zone. A Faraday cup at the beam-exit port of the chamber serves to monitor the beam current just after the interaction region, while a grounded quartz plate after this is used to monitor the beam profile. The performance test of the entire setup has been very satisfactory, and the experiments are underway.

## D. Facility for Atomic and Molecular Collisional Studies

Sankar De[1], C. P. Safvan, R. Ahuja, U. K. Rao, S. J. Venkatesh, Sunder Rao, S. K. Saini, A. Roy and P. N. Ghosh[1]

[1]Department of Physics, University of Calcutta, 92, A. P. C. Road, Kolkata- 700009

Fragmentation of molecules by slow, highly charged ions is an emerging field where coincident detection of correlated products can give direct information on dissociation dynamics. An experimental facility is developed to study such collisional phenomenon along with multiple electron capture and ionization studies of atomic targets.

In our set-up (Fig. 1), recoil ions from dissociated molecules and ejected electrons are extracted from the interaction zone by uniform electric field into their time-of-flight (TOF) spectrometers. The collision centre is defined by projectile, gas jet target and TOF spectrometers, all mutually orthogonal to each other. Fragments are separated out in recoil TOF according to their m/q and detected by a position sensitive dual micro channel plate (MCP) detector with delay line anode. Electrons on their TOF are detected by channeltron. For post collision analysis of the charge exchanged projectiles, we have set-up a parallel plate electrostatic analyser just after the collision zone. Different charge states can be separated out by varying the electric field between the two plates and the deflected ions are detected by a channeltron kept offline from the beam centre. The coincident start or stop for data acquisition can be obtained from respective channeltron signals of the electron TOF or charged exchanged projectiles [1].

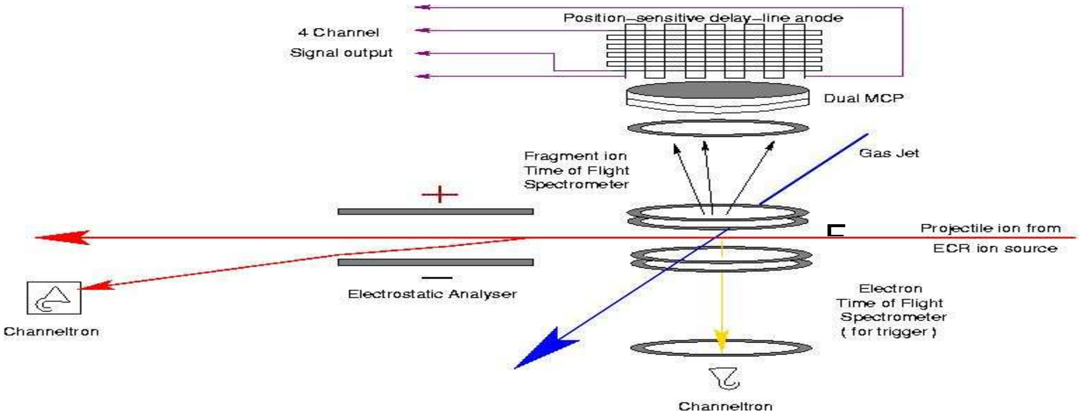

**Fig. 1 : Schematic of the experimental setup**

The first time-of-flight spectrum has been obtained with 200 KeV $N^{2+}$ beam from the ECR source with Argon as target gas. Along with the ionised atomic peaks, fragmented molecular peaks from the background gas is also observed (Fig. 2).

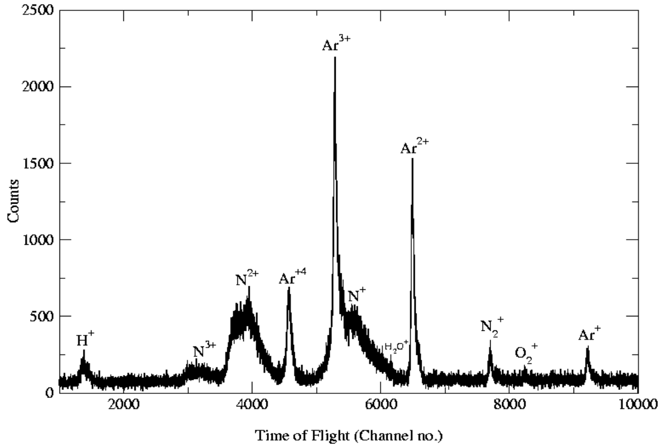

**Fig. 2 : Time of flight spectrum**

We are thankful to Dr. F. A. Rajgara of TIFR, Dr. D. Kanjilal and G. K. Padmashree for their suggestions and help in building up the setup and Jyoti for her help during the experiments.

## REFERENCES

- S. De, C. P. Safvan and P. N. Ghosh, Proc. DAE-BRNS Symp. Nucl. Phys., 46B (2003) 444

## E. Experiments at LEIBF : Generation and size characterization of micron-size liquid droplets.

G.K.Padmashree[1], C.P.Safvan, and R.Somashekar[1]

[1]Department of Studies in Physics, University of Mysore, Manasagangotri, Mysore - 570 006.

The experiments with 'liquid droplet clusters' is a novel area of research which is fascinating in its own right since microdroplets are macroclusters having bulk-like packing densities, and yet exhibit certain properties of large molecules/small clusters due to their spatial confinement. We have initiated radically new experiments to understand the interaction dynamics of droplets in their collisions with highly charged ions (HCI) of low energy (in the keV-MeV range) from the ECR ion source.

The microdroplets (of low viscosity liquids under high pressure) are generated by uniform break up of a high-velocity microjet that emerges from a vacuum-compatible piezocrystal-driven microcapillary tube that has an orifice of 10 microns (diameter). On applying a monochromatic disturbance of wavelength $\lambda = 2\ \ r_j$ ($r_j$ is the radius of the jet) symmetric about the jet axis, the microjet breaks up into a train of uniformly-sized microdroplets, with the inter-droplet spacing equal to the disturbance wavelength. The size of the droplet (spherical scatterer) is determined from the angular intensity distribution of the light due to Mie scattering.

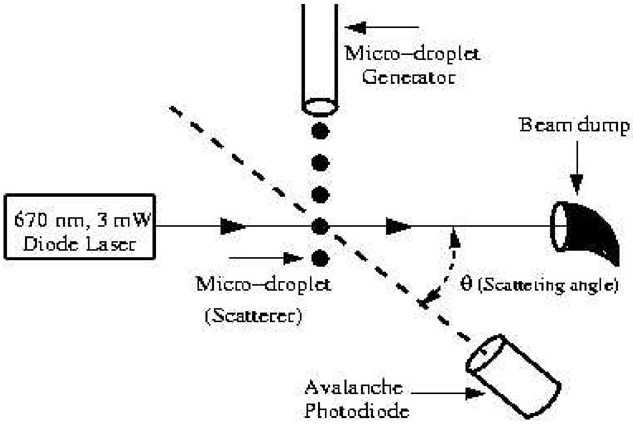

**Fig.1:Schematic of Mie scattering experimental setup - the optical nephelometer**

Mie scattering [1] is the elastic scattering of a plane EM wave, by homogeneous spheres whose size is comparable to the wavelength of the incident light. A dimensionless number called the size parameter physically represents the number of wavelengths that fit into the scatterer, and is given by $x = 2\ r/\lambda$, r is the radius of the sphere and $\lambda$ is the wavelength of incident light. The scattered intensity is a function of the extinction coefficient which in turn is a function of size parameter. Thus, a knowledge of the scattered intensity enables determination of the scatterer's size and the crux of the problem lies in determining the scattered intensities [2].

Monochromatic light of 670 nm wavelength emitted by a 3 mW diode laser was incident on liquid droplets emerging from a piezocrystal-driven microcapillary tube. The scattered light was detected by an avalanche photodiode mounted on a stepper-motor driven rotation stage that was capable of 360° rotation. Enough care was taken to optimize the signal to noise ratio by enclosing the entire setup in a black box, thereby eliminating all the stray light. An angular intensity distribution of the scattered light in the forward angles (up to 70°, in steps of $1^0$) was obtained, with the perpendicular polarization of the incident light. A PC was used to control the motion of the stepper -motor and for data acquisition through RS232 interface.

The Mie scattering routines [3,4] were employed to generate scattered intensities at different scattering angles for a variety of size parameters, and the microdroplet size has been calculated from the size parameter corresponding to the best fit of the experimental and computed intensities.

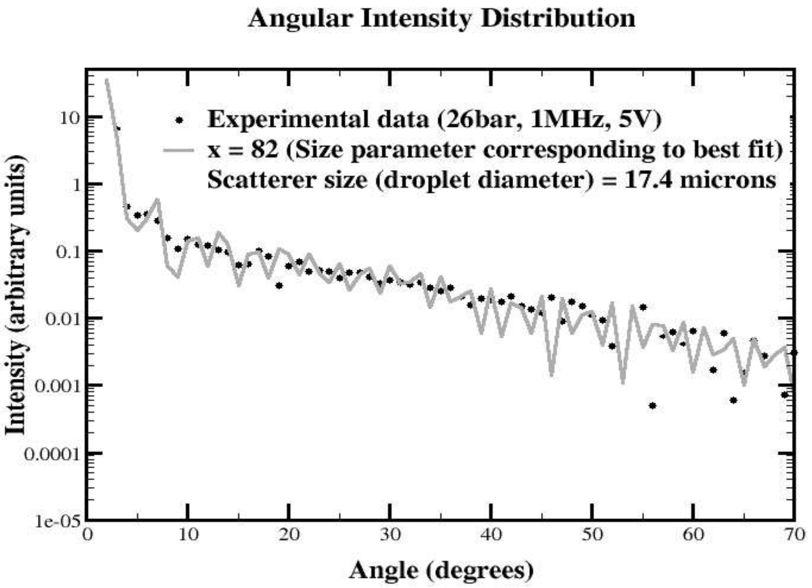

**Fig 2 : Angular intensity distribution data with the corresponding best fit**

The computed intensities for the best fit correspond to x = 82 i.e., the diameter of the scatterer is 17.4 microns. Hence, the microdroplet has a diameter of 17.4 ± 0.1 microns under the experimental conditions of 24 bar backing pressure, 5V amplitude and 1MHz frequency. We have repeated the experiment many times, and the results are reproducible. This result is in good agreement with the theoretical value of droplet diameter as obtained from the drop formation theory (18.7 microns).

## REFERENCES

- G.Mie, Ann.Physik, 2, 377, (1908)
- Light sattering by small particles, H.C. Van de Hulst, John Wiley & Sons Inc London.
- Warren Wiscombe 'Improved Mie scattering algorithms', App Opt, 19(9), 1505 - 1509 (1980)
- I. Weiner M.Rust and T.D.Donnelly, Am.J.Phys, 69 (2), 129, 2001.

## 2.6 Performance of High Temperature Superconducting Electron Cyclotron Resonance Ion Source Pkdelis

D. Kanjilal, G. O. Rodrigues, P. Kumar, C. P. Safvan, U. K. Rao, A. Mandal,
A. Roy, C. Bieth[1], S. Kantas[1] and P. Sortais[2]

[1]Pantechnik, 14000 CAEN, France
[2]Institut des Sciences Nuclaire, INS-IN2P3, Grenoble France Design of a High

### *(i) Introduction*

A new type of high temperature superconducting electron cyclotron resonance ion source (HTS-ECRIS) called PKDELIS has been designed and developed as a collaborative project. The source is operational at 14 to 18 GHz and is suitable for use on a 300 kilo volt (kV) platform with minimum requirements of electrical power and cooling water. The beam from the source will be mass analyzed on the deck using an air cooled magnet placed on the HV platform.

### *(ii) Design features*

The design of this high performance positive ion source is based on the required mass to charge ratio of ~ 7 for the high current injector (HCI) of NSC. PKDELIS is suitable to provide high current multiply charged positive ion beams for injection into the superconducting linear accelerator (SC-LINAC) after pre-accelerating the beams to matching energy using radio frequency quadrupoles and low velocity resonators. Since no cryogen can be transferred across the high potential of 300 kV, high temperature superconducting coils of Bi-2223 have been chosen to reduce the power and cooling requirements for producing the large axial magnetic fields corresponding to a frequency of 18 GHz. The HTS coils are operated at a temperature of about 20 K by using Gifford-

McMahon cryo-coolers. The calculation of the axial field profile by the POISSON group of codes using solenoid coils made of BSSCO-2223 HTS wires at an operational current density of 90 A mm$^{-2}$ has been worked out. The hexapole design is based on the design of the Halbach configuration and is made of permanent magnets comprising of Nd, Fe, and B. Surface treated magnets are to be used for high temperature and high humidity applications. The 3D calculations of hexapole fields using minimum possible values of $B_r$ have been calculated for both 24 sectors and 36 sectors. The design is aimed for maxium field using 36 wedge shaped magnets. The ion optical calculations of the extraction system in the presence of the strong axial field produced by the HTS coils has been worked out using the IGUN code. The total extraction system comprises of the plasma electrode, puller electrode, focus electrode and a last electrode with the same potential as the puller electrode. The puller electrode is polarised to a negative potential of -20 kV in order to obtain better optics. For example, trajectories of oxygen beams in various charge states, for an extraction voltage of 35 kV (bias voltage of the plasma tube) and puller voltage of -20 kV for total source current of 10 mA inside the puller electrode has been calculated.

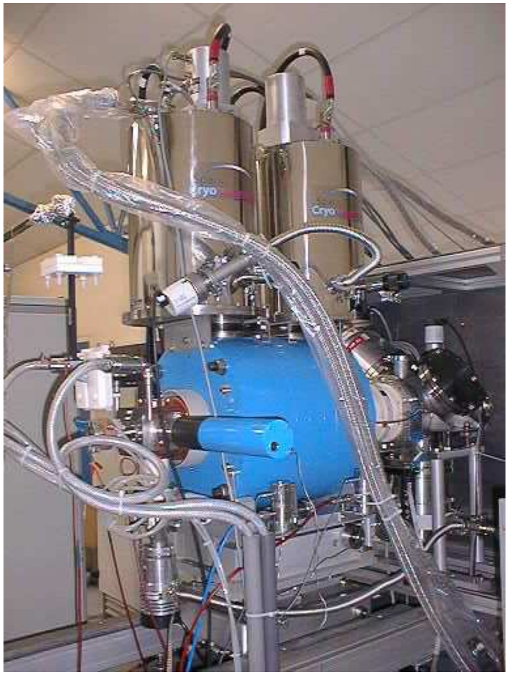

**Fig. 1 : View of the high temperature superconducting ECR ion source, PKDELIS**

### *(iii) TEST results of HTS coils and Permanent magnet hexapole*

The testing of the HTS coils were carried out at Space Cryomagnetics Ltd, UK. Each of the coils were tested stand-alone for reliability of continous operation. The cool down process for the coils takes about 12 hours to reach the operating temperature. For example, when the individual coils were excited to 150 A, the equilibrium temperatures of the coil former for the injection and extraction coils were at 22 K and 20 K respectively. The test results for both the coils were found to be comparable. The measurements show very well agreement with the simulations using POISSON and OPERA 3D. The field mapping of the hexapole was done at the factory of PANTECHNIK. The measured radial field on the chamber wall was measured to be 1.35 T. Table 1 gives an idea of the extracted beam currents for some of the optimised beams.

**Table 1: Extracted currents for various ions**

| Ion species | Rf power (Watts) | Beam curent (eμA) |
|---|---|---|
| $^{12}C^{2+}$ | 597 | 2000 |
| $^{16}O^{2+}$ | 193 | 2037 |
| $^{20}Ne^{2+}$ | 391 | 2044 |
| $^{20}Ne^{3+}$ | 391 | 1533 |
| $^{40}Ar^{4+}$ | 496 | 1023 |
| $^{40}Ar^{7+}$ | 488 | 617 |
| $^{129}Xe^{14+}$ | 614 | 157 |
| $^{129}Xe^{21+}$ | 652 | 28 |
| $^{180}Ta^{20+}$ | 426 | 65 |
| $^{180}Ta^{25+}$ | 476 | 27 |
| $^{197}Au^{21+}$ | 898 | 28 |
| $^{208}Pb^{21+}$ | 1197 | 66 |
| $^{208}Pb^{29+}$ | 738 | 12 |